Nonlinear photoionization of transparent solids: A nonperturbative theory obeying selection rules

N. S. Shcheblanov,[1,2,*] M. E. Povarnitsyn,[3,1] P. N. Terekhin,[4] S. Guizard,[2] and A. Couairon[1]
[1]*Centre de Physique Théorique, CNRS, École polytechnique, Paris-Saclay University, F-91128 Palaiseau, France*
[2]*Laboratoire des Solides Irradiés CEA-CNRS, École polytechnique, Paris-Saclay University, F-91128 Palaiseau, France*
[3]*Joint Institute for High Temperatures, RAS, 13 Bld. 2 Izhorskaya str., 125412 Moscow, Russia*
[4]*National Research Centre "Kurchatov Institute", Kurchatov Sq. 1, 123182 Moscow, Russia*
(Received 23 June 2017; revised manuscript received 19 October 2017; published 15 December 2017)

We provide a nonperturbative theory for photoionization of transparent solids, which consistently accounts for the *selection rules* related to the parity of the number of absorbed photons (*odd* or *even*). We derive closed-form analytical expressions for the photoionization rate within the two-band structure model. Our model exhibits excellent agreement with measurements for the frequency dependence of the two-photon absorption and nonlinear refractive index coefficients in sapphire and silica, two highly relevant materials for industrial applications. We demonstrate the crucial role of the interference of the transition amplitudes, which in the semiclassical limit can be interpreted in terms of interfering quantum trajectories that were disregarded in Keldysh's foundational work of laser physics [Keldysh, Sov. Phys. JETP **20**, 1307 (1965)], resulting in the violation of selection rules.

DOI: 10.1103/PhysRevA.96.063410

I. INTRODUCTION

The permanent development of high-power pulsed lasers continues to attract attention to multiphoton processes, predicted by Dirac [1] and Göppert-Mayer [2]. These processes are important for a number of applications like spectroscopy [3,4], photoemission studies [4–6], high harmonic generation in solids [7–13], or optical communications [14]. In particular, the spatially confined excitation produced by two-photon absorption (2PA) is useful for three-dimensional data storage and imaging [15–17]. Recently, a possible way towards two-photon semiconductor lasers has been proposed [18]. These successes have roused the interest in exploring applications based on three-photon absorption (3PA) [19] and higher-order multiphoton processes [20,21].

In 1964, Leonid Keldysh developed a cornerstone theory [22] dedicated to multiphoton processes. While experimental data for the multiphoton absorption coefficient were favorably compared to Keldysh's formula for the ionization probability [see Eq. (37) in Ref. [22]], several authors point out a discrepancy by as much as an order of magnitude, as well as the lack of spectrally resolved measurements [23–25]. Nevertheless, experiments were conducted in the class of transparent solids with inversion symmetry allowing for one-photon transition [26], and confirmed the frequency dependence predicted by the perturbation theory [24,27,28] for the l-photon transition rate as

$$w_l \sim \begin{cases} (l\hbar\omega - \epsilon_g)^{1/2}, & l \text{ odd}, \\ (l\hbar\omega - \epsilon_g)^{3/2}, & l \text{ even}, \end{cases} \tag{1}$$

where ϵ_g is the band gap. Equation (1) is the signature of the fundamental principle in quantum physics known as selection rules. In contrast, the Keldysh theory reduces to the expression $w_l \sim \sqrt{l\hbar\omega - \epsilon_g}$ for l odd and l even [22], therefore violating selection rules [24,28]. Possible reasons for this discrepancy were proposed by Vaidyanathan *et al.* [28], who highlighted simplifying assumptions in Keldysh's derivation with regard to the electronic band structures and oscillator strengths, and suggested to replace the approximate saddle-point integration in the Keldysh derivation by an exact integration. However, an analytical theory for photoionization rates of dielectrics that consistently obey selection rules is still missing. Modern computer simulations of laser-matter interaction use broadly the original Keldysh theory [29].

In this paper, we present an elegant solution to the critical outstanding problem of deriving rates for ionization of transparent solids by strong electromagnetic waves which consistently obey selection rules, thus improving Keldysh's theory (KLD). We show that violation of selection rules in Keldysh's theory originated in the disregard of interference between quantum trajectories. We establish closed-form analytical laws for the photoionization rates of transparent solids and demonstrate that recent measurements of two-photon absorption and nonlinear index coefficients in silica and sapphire are reproduced by our theory with excellent agreement.

II. PHOTOIONIZATION RATES

In Ref. [22], Keldysh provided a detailed description of the nonperturbative method to derive the expression for the photoionization rate using the Houston wave functions [30]. However, features such as selection rules at low intensity [27], modulation of photoionization rates with intensity caused by the dynamic Stark effect, and the calculation procedure of matrix elements have not been discussed. Keldysh used approximations comprising (i) the matrix element approximation and (ii) details concerning integral calculation. In this connection we refer the reader to the recent Letters [31,32] also dedicated to the approximations in Keldysh's theory. These papers deal mostly with approximations of the band structure to unravel the difference between semiconductors and dielectrics. Here, we focus on obeying of the selection rules.

A. Derivation of photoionization rates

We start from Eq. (27) in Keldysh's work [22] for the transition rate w_{pi} from an initial state [valence band $\epsilon_v(\mathbf{p})$]

*nikita.shcheblanov@polytechnique.edu

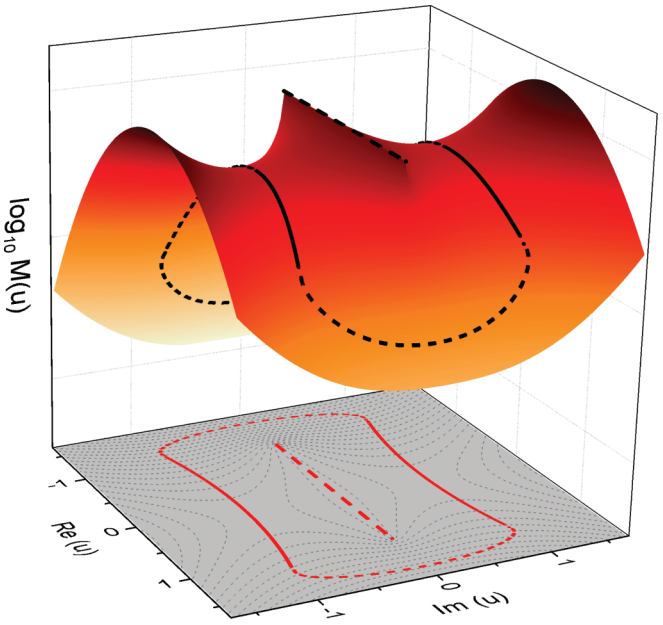

FIG. 1. Integration contour applied in Eq. (4). The integral along the real axis is indicated by a dashed line and the blown-up contour $\mathcal{C}$ is the solid line. The surface and contour lines refer to the value of $M(u)$.

to a final state [conduction band $\epsilon_c(\mathbf{p})$; gap structure $\epsilon_{cv}(\mathbf{p}) = \epsilon_c(\mathbf{p}) - \epsilon_v(\mathbf{p})$] due to the harmonic field $\boldsymbol{\mathcal{E}}_L(t) = \boldsymbol{\mathcal{E}}\cos(\omega t)$ with amplitude $\mathcal{E}$ and frequency ω:

$$w_{pi} = \frac{2\pi}{\hbar}\int \frac{d\mathbf{p}}{(2\pi\hbar)^3}|\mathcal{L}_{cv}(\mathbf{p})|^2 \sum_l \delta(\overline{\epsilon_{cv}(\mathbf{p})} - l\hbar\omega). \quad (2)$$

The quasienergy is expressed using the canonical momentum $\mathbf{p}(\tau) = \mathbf{p} + \frac{e\boldsymbol{\mathcal{E}}}{\omega}\sin\tau$, with $\tau = \omega t$, as

$$\overline{\epsilon_{cv}(\mathbf{p})} = \frac{1}{2\pi}\int_{-\pi}^{\pi} \epsilon_{cv}(\mathbf{p}(\tau))d\tau, \quad (3)$$

and the matrix element $\mathcal{L}_{cv}$ of the optical transition can be defined as an integral over a closed contour $\mathcal{C}$ [enclosing the interval $(-1,1)$; see Figs. 1 and 2] in the variable $u = \sin\omega t$ [see Eq. (29) in Ref. [22]; $\mathbf{p}(u) = \mathbf{p} + e\boldsymbol{\mathcal{E}}u/\omega$]:

$$\mathcal{L}_{cv}(\mathbf{p}) = \frac{1}{2\pi}\oint_{\mathcal{C}} \mathcal{V}_{cv}(\mathbf{p}(u))e^{iS(u)}du, \quad (4)$$

where $\mathcal{V}_{cv}(\mathbf{p}) = i\hbar\int u^{c*}_{\mathbf{p}}(\mathbf{r})e\boldsymbol{\mathcal{E}}\nabla_{\mathbf{p}}u^{v}_{\mathbf{p}}(\mathbf{r})d\mathbf{r}$ is the optical matrix element, $u^{c,v}_{\mathbf{p}}(\mathbf{r})$ are periodic functions with the translation symmetry of the lattice, and $S(u)$ is the classical action:

$$S(u) = \frac{1}{\hbar\omega}\int_0^u \frac{\epsilon_{cv}(\mathbf{p}(v))}{\sqrt{1-v^2}}dv. \quad (5)$$

We note that the optical matrix elements do not vanish for arbitrarily small photon wave vectors; hence we can use a two-band model for the calculation [24,27,31,32]. In Ref. [22], the Kane law [33] was considered:

$$\epsilon_{cv}(\mathbf{p}) = \epsilon_g\left(1 + \frac{\mathbf{p}^2}{m_r\epsilon_g}\right)^{1/2}, \quad (6)$$

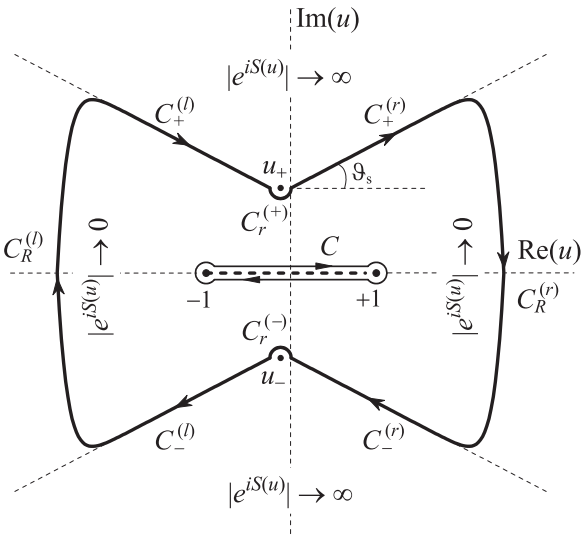

FIG. 2. Integration contour for $\mathcal{L}_{cv}$ in the u domain is depicted. The poles of $\mathcal{V}_{cv}$ lie at $u = u_\pm$ and there is a branch cut between $-1 < u < +1$ on the real axis. The contours $\mathcal{C}_R^{(r)}$ and $\mathcal{C}_R^{(l)}$ are used to connect the contours $\mathcal{C}_\pm^{(r)}$ and $\mathcal{C}_\pm^{(l)}$ at infinity.

where m_r is the reduced mass defined by $m_r^{-1} = m_c^{-1} + m_v^{-1}$, m_c and m_v are the effective masses for the conduction band and the valence band, respectively. Hence the quasienergy is

$$\overline{\epsilon_{cv}(\mathbf{p})} = \frac{2\epsilon_g}{\pi}\left[\frac{\mathrm{E}(\gamma_1)}{\gamma_2} + \frac{\gamma_2}{2}(\mathrm{E}(\gamma_1)\,x^2 + \mathrm{K}(\gamma_1)\,y^2)\right], \quad (7)$$

where $\gamma = \omega\sqrt{m_r\epsilon_g}/(e\mathcal{E})$ denotes the Keldysh parameter, $\gamma_1 = (1+\gamma^2)^{-1/2}$, $\gamma_2 = \gamma(1+\gamma^2)^{-1/2}$, $x^2 = p_\parallel^2/(m_r\epsilon_g)$ and $y^2 = p_\perp^2/(m_r\epsilon_g)$ are dimensionless variables, and the functions K and E are the complete elliptic integrals of the first and second kind.

The presence of a large factor in the exponent in Eq. (4) allows us to calculate the integral $\mathcal{L}_{cv}$ over u by a method similar to the conventional *saddle-point method*. Here, we unravel the key aspects of the method to calculate the photoionization (PI) rate, different from Keldysh's theory but consistent with the *selection rules*.

The integration path in Eq. (4) must be treated with some care as was shown by authors in Refs. [34,35]. This is due to the substitution $u = \sin\omega t$ which is not straightforward due to the lack of a bijective connection between u and ωt.

In order to further investigate suitable deformations of the integration contour, we consider the following real function $M(u)$ defined in the complex u plane:

$$M(u) = |e^{iS(u)}|. \quad (8)$$

To simplify our consideration we deal with a parabolic band structure:

$$\epsilon_{cv}(\mathbf{p}) = \epsilon_g\left(1 + \frac{\mathbf{p}^2}{2m_r\epsilon_g}\right) \quad (9)$$

and, hence, the corresponding quasienergy is

$$\overline{\epsilon_{cv}(\mathbf{p})} = \epsilon_g\left[\left(1 + \frac{1}{4\gamma^2}\right) + \frac{x^2+y^2}{2}\right]. \quad (10)$$

Now we rewrite Eq. (5) at a momentum $\mathbf{p}_l$ corresponding to the lth term of Eq. (2). Thus we can find $S(u)$ as

$$S(u) = l\ \arcsin u - \frac{\epsilon_g}{2\hbar\omega}\left(\frac{u}{2\gamma^2} - \frac{2x}{\gamma}\right)\sqrt{1-u^2}. \quad (11)$$

Since the exponent in Eq. (4) involves the function $\arcsin u$ [see Eq. (11)], we must use functions of u such that, as $\mathrm{Re}(u) \to 0$,

$$\mathrm{Re}(\arcsin u) \to \begin{cases} -\pi, & u \in \text{lower left quadrant}, \\ 0, & u \in \text{upper half-plane}, \\ +\pi, & u \in \text{lower right quadrant}. \end{cases} \quad (12)$$

The square root is usually defined to possess a non-negative real part.

As shown in Figs. 1 and 2, there are two saddle points u_s with opposite imaginary parts, distinguished by the index $s := \{\pm\}$ which denotes the sign of $\mathrm{Im}(u_s)$. The saddle points are determined by the condition $\epsilon_{cv}(\mathbf{p}(u)) = 0$. They provide the main contribution to the integral $\mathcal{L}_{cv}$. For the parabolic law, the saddle points u_s are

$$u_\pm = -\gamma\, x \pm i\gamma\sqrt{2+y^2} \quad (13)$$

and for the Kane law

$$u_\pm = -\gamma\, x \pm i\gamma\sqrt{1+y^2}. \quad (14)$$

Unlike the conventional saddle-point method, the function $\epsilon_{cv}(\mathbf{p}(u))$ is not analytic and the preexponential factor $\mathcal{V}_{cv}(\mathbf{p}(u))$ has poles at these points. The character of the singularities was considered in detail by Keldysh [36] and Krieger [37]. Taking these features into account, we deform the integration contour $\mathcal{C}$ with respect to u as shown by the solid contour in Fig. 2. We deform the contour from the real axis to the lower and upper half-planes so that it passes around the points u_s along semicircles of infinitesimal small radius r (via the integration paths $\mathcal{C}_r^{(s)}$) and goes along the rays $\mathcal{C}_s^{(r)}$ and $\mathcal{C}_s^{(l)}$, where the contours $\mathcal{C}_R^{(r)}$ and $\mathcal{C}_R^{(l)}$ are used to connect the contours $\mathcal{C}_s^{(r)}$ and $\mathcal{C}_s^{(l)}$ at infinity. A simple analysis shows that the integrals $\mathcal{L}_{cv}$ along the $\mathcal{C}_R^{(r)}$ and $\mathcal{C}_R^{(l)}$ contours vanishes (see Fig. 1). In order to evaluate the remaining integrals ($\mathcal{C}_s$: $\mathcal{C}_s^{(r)}$, $\mathcal{C}_r^{(s)}$, and $\mathcal{C}_s^{(l)}$), we use $u = u_s + \xi$, and represent the function $S(u)$ in the form

$$S(u) = \int_0^{u_s} + \int_{u_s}^{u_s+\xi} = S(u_s) + S_s(\xi). \quad (15)$$

By expanding the preexponential factor in Eq. (4) near u_s, we obtain in the frame of a two-band model [36,37] for solids where one-photon transition is allowed [26]

$$\mathcal{V}_{cv}(\mathbf{p}(u)) \sim \frac{\mathrm{sgn}(u_s)}{4i(u-u_s)}. \quad (16)$$

Thus, accounting for $\xi = u - u_s$, we obtain

$$\mathcal{L}_{cv}(\mathbf{p}) \sim \frac{1}{4}\sum_s \mathrm{sgn}(u_s) e^{iS(u_s)} \int_{\mathcal{C}_s} \frac{e^{iS_s(\xi)}}{\xi} d\xi. \quad (17)$$

In order to complete the integration in Eq. (17), the dispersion law $\epsilon_{cv}(\mathbf{p})$ must be specified. The essential difference from the Keldysh description is, however, the fact that the dispersion law must be specified at this stage rather than at a stage of integration over momentum $\mathbf{p}$ in Eq. (2). This is due to the necessity to determine the Stokes (steepest-descent) line angles.

Using the parabolic law Eq. (9) in $S_s(\xi)$ at $\mathbf{p} = 0$ and neglecting terms of higher order in ξ, we obtain

$$iS_\pm(\xi) \approx \pm\frac{\epsilon_g}{2\hbar\omega}\left\{\sqrt{2}\frac{\xi^2 e^{i\pi}}{\gamma\sqrt{1+2\gamma^2}} + O(\xi^3)\right\}. \quad (18)$$

From the change of variable $\xi = r\ \exp(i\vartheta)$, we find that the steepest-descent lines are the rays corresponding to ϑ_s and $-\pi - \vartheta_s$. Thus we have $\vartheta_s = 0$ and $-\pi - \vartheta_s = -\pi$; hence the angle between the steepest descent lines is π.

It is easy to show that the integrals along the rays $\mathcal{C}_s^{(r)}$ and $\mathcal{C}_s^{(l)}$ cancel each other. On the left ray of the upper half-plane $\xi = r\ \exp(-i\pi)$ and $d\xi = \exp(-i\pi)dr$; then

$$\int_{\mathcal{C}_+^{(l)}} \frac{e^{iS_+(\xi)}}{\xi} d\xi = \int_{-R}^{-\rho} \frac{e^{\tilde{a}(-r)^2}}{r} dr \to -\int_0^{+\infty} \frac{e^{\tilde{a}r^2}}{r} dr. \quad (19)$$

On the right ray of the upper half-plane $\xi = r\ \exp(i\pi)$ and $d\xi = \exp(i\pi)dr$; then

$$\int_{\mathcal{C}_+^{(r)}} \frac{e^{iS_+(\xi)}}{\xi} d\xi = \int_{\rho}^{R} \frac{e^{\tilde{a}(-r)^2}}{r} dr \to \int_0^{+\infty} \frac{e^{\tilde{a}r^2}}{r} dr. \quad (20)$$

Similar relations hold for the lower saddle point, u_-. Thus both integrals along the rays $\mathcal{C}_s^{(r)}$ and $\mathcal{C}_s^{(l)}$ are opposite; hence they cancel each other.

Using the Kane law in $S_s(\xi)$ at $\mathbf{p} = 0$ and neglecting terms of higher order in ξ, we obtain

$$iS_\pm(\xi) \approx \pm\frac{\epsilon_g}{2\hbar\omega}\left\{\frac{2\sqrt{2}}{3}\frac{\xi^{3/2} e^{i3\pi/4}}{\sqrt{\gamma(1+\gamma^2)}} + O(\xi^{5/2})\right\}. \quad (21)$$

From the change of variable $\xi = r\ \exp(i\vartheta)$, we find that the steepest-descent lines are the rays corresponding to $\vartheta_s = \pi/6$ and $-\pi - \vartheta_s = -7\pi/6$. Thus the angle between the lines of steepest descent is $4\pi/3$. It is also easy to show that the integrals along the rays $\mathcal{C}_s^{(r)}$ and $\mathcal{C}_s^{(l)}$ cancel each other in this case.

In fact, the integration in Eq. (17) reduces for both band structures to bypassing singularities u_s, along semicircles of infinitesimal small radius r (via the integration paths $\mathcal{C}_r^{(s)}$ which are the only contributing paths). Hence the angle between the rays determines the final contribution to $\mathcal{L}_{cv}$ as follows:

$$\mathcal{L}_{cv}(\mathbf{p}) \sim \frac{1}{4}\sum_s \mathrm{sgn}(u_s)(\pi + 2\vartheta_s) e^{iS(u_s)}. \quad (22)$$

Thus, for the parabolic law, we find that the contribution to Eq. (4) made by each of the saddle points is equal to

$$\pm\frac{\hbar\omega}{8}\exp\{iS(u_\pm)\} \quad (23)$$

and for the Kane law we have the following:

$$\pm\frac{\hbar\omega}{6}\exp\{iS(u_\pm)\}. \quad (24)$$

Saddle points $u_\pm$ are in the upper left and lower left quadrants (see Fig. 2). Therefore, the argument $iS(u_s)$ of the exponential function in Eq. (22) and also the quasienergy $\overline{\epsilon_{cv}}$ in Eq. (2)

can be calculated exactly by using the analytical continuation of functions in the complex plane such as Eq. (12) for the parabolic case. We represent $S(u_s)$ as $\varphi_0 + i\varphi_s$.

By using the delta function from Eq. (2) with quasienergy Eq. (10), for the parabolic case, we obtain

$$\varphi_0 = -\frac{\epsilon_g}{\hbar\omega}\left\{\frac{l\hbar\omega}{\epsilon_g}\sinh^{-1}(\sqrt{2}\gamma) - \frac{x^2}{\sqrt{2}}\frac{\gamma}{\sqrt{1+2\gamma^2}} - \frac{\sqrt{1+2\gamma^2}}{2\sqrt{2}\gamma}\right\} \tag{25}$$

and

$$\varphi_+ = \varphi = -x\frac{\epsilon_g}{\hbar\omega}\left(\frac{1}{\gamma} - \frac{\sqrt{1+2\gamma^2}}{\gamma}\right). \tag{26}$$

For the Kane law the result is obtained after an expansion of $S(u_s)$ at $\mathbf{p} = 0$, as suggested in Ref. [22], and reads

$$\varphi_0 = -\frac{\epsilon_g}{\hbar\omega}\left\{\frac{1}{\gamma_2}[\mathrm{K}(\gamma_2) - \mathrm{E}(\gamma_2)] + \frac{x^2\gamma_2}{2}[\mathrm{K}(\gamma_2) - \mathrm{E}(\gamma_2)] + \frac{y^2\gamma_2}{2}\mathrm{K}(\gamma_2)\right\} \tag{27}$$

and

$$\varphi_+ = \varphi = \frac{x}{2}\frac{\epsilon_g}{\hbar\omega}\,\mathrm{arccot}\left(\frac{1}{2\gamma} - \frac{\gamma}{2}\right), \tag{28}$$

whereas $\varphi_- = -l\pi - \varphi$. In result, due to the summation in Eq. (22), the contribution to the integral $\mathcal{L}_{cv}$ from both saddle points located in the complex plane acquires a phase factor:

$$\mathcal{L}_{cv}(\mathbf{p}) \sim (e^{i\varphi(\mathbf{p})} - e^{-il\pi - i\varphi(\mathbf{p})}) \sim \sin(\pi l/2 + \varphi). \tag{29}$$

Indeed, this interference effect is sensitive to the phase of the electron wave function. Thus we can see that for solids with an allowed one-photon transition, even-photon absorption is forbidden at $(l\hbar\omega - \epsilon_g) \approx 0$ (i.e., $\varphi \sim 0$), as evidenced by the perturbation theory [27].

By substituting the obtained expression for $\mathcal{L}_{cv}$ in Eq. (2) and summing over momentum, we obtain a closed-form solution for the total probability of an interband transition per unit time and per unit volume in transparent solids within the two-band model:

$$w_{pi}(\omega) = \sum_{l=l_{pi}} w_l^{pi}(\omega), \tag{30}$$

where $l_{pi} = [\nu + 1]$ denotes the minimum number of photons involved in the transition (the symbol $[\nu]$ denotes the integer part of a number ν) and $\nu = \bar{\epsilon}_g/\hbar\omega$. The quasienergy $\bar{\epsilon}_g$ will be specified from the band-gap knowledge. The corresponding relative PI rate is expressed as a function of frequency and the Keldysh parameter of the form:

$$w_l^{pi} = \omega\left(\frac{m_r\omega}{\hbar}\right)^{3/2} f_1(\gamma)Q_l(\gamma,\nu)\exp(-\alpha l_{pi}), \tag{31}$$

where the function

$$Q_l(\gamma,\nu) = f_2(\gamma)\phi_l(\sqrt{\beta(l-\nu)})\exp\{-\alpha(l-l_{pi})\}, \tag{32}$$

TABLE I. Band-structure-dependent quantities.

	Parabolic	Kane
$\bar{\epsilon}_g$	$\epsilon_g(1+\frac{1}{4\gamma^2})$	$\frac{2\epsilon_g \mathrm{E}(\gamma_1)}{\pi\gamma_2}$
α	$2\,\sinh^{-1}(\sqrt{2}\gamma) - \beta$	$\frac{\pi[\mathrm{K}(\gamma_2)-\mathrm{E}(\gamma_2)]}{\mathrm{E}(\gamma_1)}$
β	$\frac{2\gamma}{\sqrt{\gamma^2+1/2}}$	$\frac{\pi^2}{2\mathrm{K}(\gamma_1)\mathrm{E}(\gamma_1)}$
f_1	$\frac{\exp(-\Theta\nu)}{8\pi}$	$\frac{2}{9\pi\gamma_2^{3/2}}$
f_2	$\sqrt{\frac{2}{\beta}}$	$\sqrt{\frac{\pi}{2\mathrm{K}(\gamma_1)}}$
a	$\sqrt{\frac{2\epsilon_g}{\hbar\omega}}\frac{2^{3/2}\gamma-\beta}{\gamma\beta^{3/2}}$	$\sqrt{\frac{\epsilon_g \mathrm{K}(\gamma_1)}{2\pi\hbar\omega\gamma_2}}\,\mathrm{arccot}\,(\frac{1-\gamma^2}{2\gamma})$
Θ	$\frac{2\beta\gamma^2}{1+4\gamma^2}$	

and the function ϕ_l is

$$\phi_l(z) = e^{-z^2}\int_0^z 2\,\sin^2\left(\frac{\pi l}{2} + ay\right)e^{y^2}dy. \tag{33}$$

Photoionization rates Eqs. (30)–(33) are generally valid from the multiphoton to the tunneling regime for both the parabolic and the Kane band structures, provided the corresponding band-structure-dependent quantities $\bar{\epsilon}_g$, α, β, $f_1(\gamma)$, $f_2(\gamma)$, and a are introduced; see Table I.

B. Multiphoton regime

We present here expressions corresponding to $\gamma \gg 1$ (multiphoton regime) in order to directly verify the *selection rules*. In the case of a parabolic band structure, the corresponding PI rate is given by

$$w_{pi}^P = \frac{\omega}{4\pi}\left(\frac{m_r\omega}{\hbar}\right)^{3/2}\phi_{l_{pi}}(\sqrt{2(l_{pi}-\nu)}) \times \exp(l_{pi})\left(\frac{1}{8\gamma^2}\right)^{l_{pi}}. \tag{34}$$

In the case of the Kane band structure, the corresponding PI rate per unit of volume is given by

$$w_{pi}^K = \frac{4\omega}{9\pi}\left(\frac{m_r\omega}{\hbar}\right)^{3/2}\phi_{l_{pi}}(\sqrt{2(l_{pi}-\nu)}) \times \exp(2l_{pi})\left(\frac{1}{16\gamma^2}\right)^{l_{pi}}. \tag{35}$$

A small z expansion of $\phi_l(z)$ gives

$$\phi_{l_{pi}} \approx \begin{cases}\sqrt{2}(l_{pi}-\nu)^{1/2}, & l_{pi}\ \text{odd},\\ \frac{2\sqrt{2}a^2}{3}(l_{pi}-\nu)^{3/2}, & l_{pi}\ \text{even},\end{cases} \tag{36}$$

where a, in the parabolic case, reads as follows:

$$a = \sqrt{\frac{2\epsilon_g}{\hbar\omega}}, \tag{37}$$

and a, in the case of the Kane law, reads as follows:

$$a = \frac{\pi}{2}\sqrt{\frac{\epsilon_g}{\hbar\omega}}. \tag{38}$$

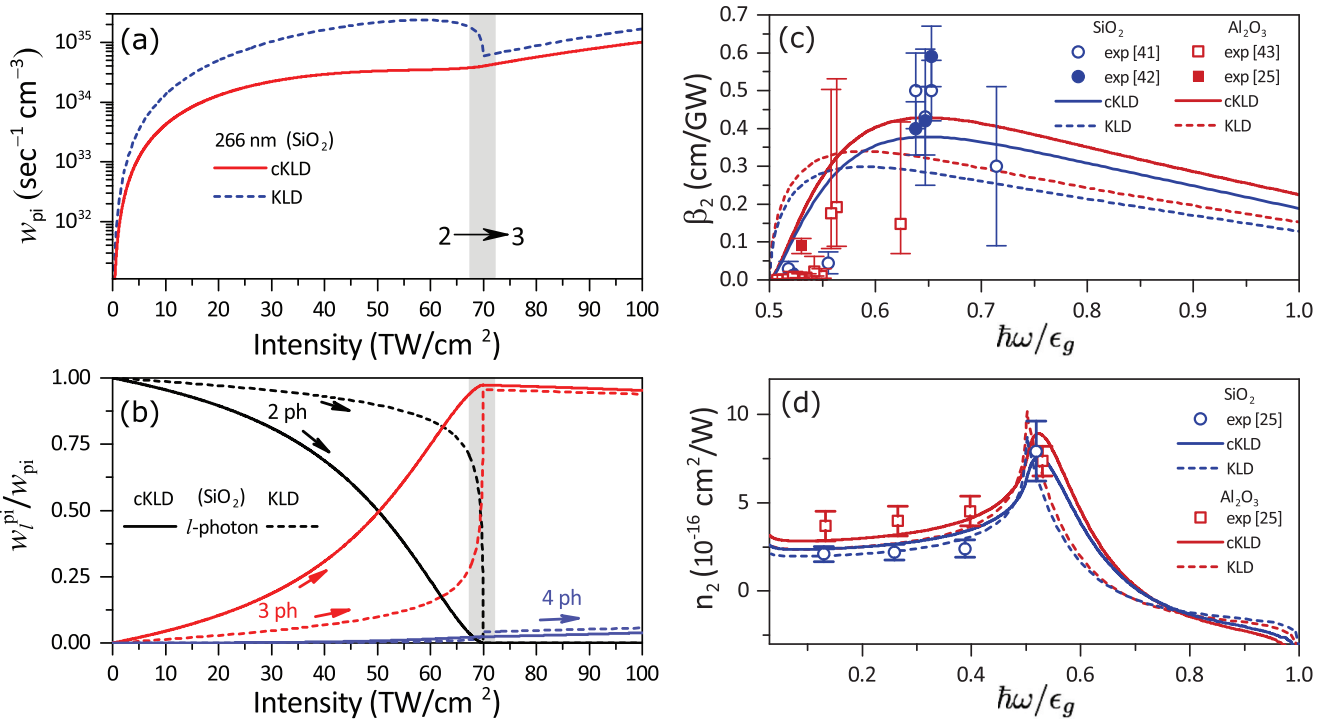

FIG. 3. Left column—comparison between the original Keldysh and the corrected Keldysh formulas of photoionization rates in SiO_2 as functions of laser intensity at the wavelength of 266 nm. Solid curves correspond to cKLD formula and dashed curves reproduce the KLD formula. (a) Total PI rate. (b) Relative contribution of two- (black), three- (red), and four-photon (blue) processes to photoionization. The channel-closure region at $I \approx 70\,\mathrm{TW\,cm^{-2}}$ is indicated by the gray shaded area, (a) and (b), and horizontal arrow, (a). Right column—comparison between theory (curves) and experiment (markers) in SiO_2 (blue) and Al_2O_3 (purple). Solid and dashed curves are numerical results via cKLD and KLD theory, respectively. (c) 2PA coefficient β_2. Fused silica (empty circles) and crystalline quartz (filled circles) [41,42], Al_2O_3 [43] (empty squares), and [25] (filled square). (d) Experimental and numerical nonlinear refractive index n_2. Experimental data are taken from [25]: empty circles for SiO_2 and empty squares for Al_2O_3. *Notes*: Refs. [44,45].

In Eqs. (34)–(36), the quantity $\nu \to \epsilon_g/\hbar\omega$ as $\gamma \gg 1$; hence the dominant dependence upon the field amplitude, determined by $\gamma^{-2I_{pi}}$, is retrieved for both PI rates, Eqs. (34) and (35).

The interference effect underlined in Eq. (29) takes place from the multiphoton to the tunneling regime. However, we note that in the tunneling regime, photoionization rates become weakly dependent on frequency leading to the suppression of the frequency signature of selection rules.

C. Interpretation of results

Keldysh supposed [22] that "the term in Eq. (36) [$iS(u_s)$ in our notations], which is linear in x [dimensionless momentum], will henceforth be left out, for when account is taken of both saddle-points it gives rise in $\mathcal{L}_{cv}$ to a rapidly oscillating factor of the type $2\cos(ax)$, which reduces after squaring and integrating with respect to x to a factor 2, which we can take into account directly in the final answer." However, we show that it is precisely this assumption that violates the selection rules [see Eq. (1)]. The argument $iS(u_s)$ of the exponential function in Eq. (22) must indeed be preserved. Due to the summation in Eq. (22) the contribution to the integral $\mathcal{L}_{cv}$ from both saddle points located in the complex plane acquires a phase factor. This phase factor is a signature for the interference of the transition amplitudes, the proper treatment of which is responsible for obeying the selection rules.

An interference factor of a similar nature was first obtained by Perelomov *et al.* [38] in 1966 for the PI rate of *atoms*. However, the idea that an interference effect is important for understanding selection rules has been put forward only recently by Popruzhenko *et al.* [39,40] who derived a quantum equation for the photoionization rate and interpreted it in terms of quantum interference of scattering amplitudes using the self-consistent Born approximation and the Keldysh technique [39]. The summation Eq. (22) can thus be interpreted in terms of interfering quantum trajectories. A key feature of our approach is simplicity since the matrix element can be directly evaluated for the two-band model in solids; see Eq. (16).

A simple analysis [see Eq. (36)] shows that in the perturbation regime corresponding to low intensities ($\gamma \gg 1$), the rates Eqs. (31)–(33) are reduced to Eq. (1) via a small z expansion of $\phi_l(z)$ and $z = \sqrt{\beta(l-\nu)}$:

$$\phi_l \sim \begin{cases} (l\hbar\omega - \epsilon_g)^{1/2}, & l \text{ odd}, \\ (l\hbar\omega - \epsilon_g)^{3/2}, & l \text{ even}, \end{cases} \tag{39}$$

i.e., obey the selection rules for any band structure approximation, Kane or parabolic, and hence agree with the perturbation theory. This result significantly improves Keldysh's theory while preserving its analytic nature; hence rates Eqs. (31)–(33) can be plugged into modern computer simulations of laser-matter interaction with moderate computational cost [29].

III. COMPARISON OF 2PA COEFFICIENT AND REFRACTIVE INDEX WITH EXPERIMENTS

In order to compare the results of the corrected theory with experiment, we choose SiO_2 and Al_2O_3, two highly relevant materials for industrial applications. The band structure of these wide-band gap insulators [46,47] can be well approximated by a two-band model with only two parameters, the reduced mass m_r and the band gap ϵ_g. We use $m_r = 0.9m_0$ and $\epsilon_g = 9.0$ eV for SiO_2 and $m_r = 0.35m_0$ and $\epsilon_g = 8.8$ eV for Al_2O_3.

Figure 3(a) shows the dependence of the PI rate per unit volume on laser intensity, for SiO_2 at the laser wavelength 266 nm, as calculated from the KLD theory and the cKLD model. The cusp at $\approx$70 TW/cm^2 is the signature of two- to three-photon absorption transition in the Keldysh formula, and is due to the energy shortage as the electron ponderomotive energy grows up with increasing laser field amplitude (the dynamic Stark effect), and thus the probability of photoionization decreases sharply highlighting the signature of channel closing [48,49]. As can be seen in Fig. 3(a), this cusp is no longer present in our corrected cKLD model reflecting the proper *superposition* of channels, 2PA and 3PA, respectively. In Fig. 3(b) we evaluate the relative contribution of multiphoton processes (channels) to the total photoionization rate. For the KLD model, the contribution of 2PA vanishes at $\approx$70 TW/cm^2, i.e., the 2PA channel closes, while the contribution of 3PA abruptly increases. For the cKLD model, a smooth transition from 2PA to 3PA is obtained: the contribution of 3PA compensates for the attenuation of the 2PA process.

By taking into consideration only the 2PA process, which is valid in the limit of low laser intensities, we compare theoretical predictions for the 2PA coefficient β_2 calculated from the KLD and cKLD models with measurements for SiO_2 [41,42] and recent data for Al_2O_3 [43]; see Fig. 3(c). The improved Keldysh model, cKLD, matches better with the experimental findings, especially, in the vicinity of the transition from 2PA to 3PA ($\hbar\omega/\epsilon_g \approx 0.5$), where the Keldysh model overestimates the absorption rate by a factor of $\sim$10, and further highlights and confirms the selection rules signature. The application of the Kramers-Kronig relation to the imaginary part of the permittivity gives the frequency dependence of the complex dielectric function $\varepsilon(\omega) = \varepsilon_r(\omega) + i\varepsilon_i(\omega)$, and thus allows us to derive the dispersion curves of the nonlinear refractive index $n_2(\omega)$:

$$n_2(\omega)I = \mathrm{Re}(\sqrt{\varepsilon(\omega)}) - n_0(\omega),$$

where $n_0(\omega)$ is the linear index approximated by a three-term Sellmeier dispersion equation for SiO_2 [50], Al_2O_3 [51], and $I = \epsilon_0 c n_0 \mathcal{E}^2/2$ is the laser intensity in the bulk. Dispersion curves for the nonlinear refractive index n_2 are shown in Fig. 3(d), where we present the comparison of the cKLD and KLD models with measurements [25], demonstrating again excellent agreement. As can be seen, both models give similar behavior except for the sharp peak (resonancelike behavior) at half the band gap energy, where Keldysh's model exhibits a cusp originating from the omission discussed above, whereas the corrected model yields a significant improvement. The fact that the photoionization rates obey the selection rules, Eq. (1), leads to a correct frequency dependence. In the 2PA case, the original Keldysh expression overestimates n_2 [see Fig. 3(d)] in the vicinity of the resonance due to the incorrect frequency dependence of photoionization rates introduced in the Kramers-Kronig relation [see Fig. 3(c)]. Our expression for photoionization rates differs in its frequency dependence because it obeys the selection rules; thus it gives less contribution to n_2 in this range and a higher contribution out of resonance.

IV. CONCLUSION

We derived a closed analytical expression for the photoionization rate of transparent solids that obey selection rules. Our model relies on appropriate corrections to Keldysh's theory so as to take into account the classical effect caused by interference between quantum trajectories and reduces to the equivalent results of perturbation theory. The results yield excellent agreement with experimental measurements of the two-photon absorption coefficient β_2 as well as nonlinear refractive index n_2 for materials Al_2O_3 and SiO_2.

ACKNOWLEDGMENTS

The authors thank S. Popruzhenko and N. Shvetsov-Shilovski for useful discussions. M.E.P. acknowledges support of the CNRS (France). N.S.S. and M.E.P. are grateful to the Russian Foundation for Basic Research (Project No. 16-02-00266) for financial support.

[1] P. A. M. Dirac, Proc. R. Soc. A **114**, 710 (1927).
[2] M. Göppert-Mayer, Ann. Phys. (Berlin) **401**, 273 (1931).
[3] V. M. Axt and T. Kuhn, Rep. Prog. Phys. **67**, 433 (2004).
[4] U. Bovensiepen and M. Ligges, Science **353**, 28 (2016).
[5] A. Damascelli, Z. Hussain, and Z.-X. Shen, Rev. Mod. Phys. **75**, 473 (2003).
[6] R. Pazourek, S. Nagele, and J. Burgdörfer, Rev. Mod. Phys. **87**, 765 (2015).
[7] T.-Y. Du and X.-B. Bian, Opt. Express **25**, 151 (2017).
[8] N. Tancogne-Dejean, O. D. Mücke, F. X. Kärtner, and A. Rubio, Phys. Rev. Lett. **118**, 087403 (2017).
[9] T. Tamaya, A. Ishikawa, T. Ogawa, and K. Tanaka, Phys. Rev. Lett. **116**, 016601 (2016).
[10] G. Vampa, T. Hammond, N. Thiré, B. Schmidt, F. Légaré, C. McDonald, T. Brabec, and P. Corkum, Nature (London) **522**, 462 (2015).
[11] G. Vampa, C. R. McDonald, G. Orlando, D. D. Klug, P. B. Corkum, and T. Brabec, Phys. Rev. Lett. **113**, 073901 (2014).
[12] T. Higuchi, M. I. Stockman, and P. Hommelhoff, Phys. Rev. Lett. **113**, 213901 (2014).
[13] S. Ghimire, A. D. DiChiara, E. Sistrunk, P. Agostini, L. F. DiMauro, and D. A. Reis, Nat. Phys. **7**, 138 (2011).
[14] G. Von Freymann, A. Ledermann, M. Thiel, I. Staude, S. Essig, K. Busch, and M. Wegener, Adv. Funct. Mater. **20**, 1038 (2010).
[15] D. A. Parthenopoulos and P. M. Rentzepis, Science **245**, 843 (1989).

[16] W. Denk, J. H. Strickler, and W. W. Webb, Science **248**, 73 (1990).
[17] B. H. Cumpston, S. P. Ananthavel, S. Barlow, D. L. Dyer, J. E. Ehrlich, L. L. Erskine, A. A. Heikal, S. M. Kuebler, I.-Y. S. Lee, D. McCord-Maughon, J. Qin, H. Röckel, M. Rumi, X.-L. Wu, S. R. Marder, and J. W. Perry, Nature (London) **398**, 51 (1999).
[18] M. Reichert, A. L. Smirl, G. Salamo, D. J. Hagan, and E. W. Van Stryland, Phys. Rev. Lett. **117**, 073602 (2016).
[19] G. S. He, P. P. Markowicz, T.-C. Lin, and P. N. Prasad, Nature (London) **415**, 767 (2002).
[20] J. Zhang, M. Gecevičius, M. Beresna, and P. G. Kazansky, Phys. Rev. Lett. **112**, 033901 (2014).
[21] C. Kerse, H. Kalaycıoğlu, P. Elahi, B. Çetin, D. K. Kesim, Ö. Akçaalan, S. Yavaş, M. D. Aşık, B. Öktem, H. Hoogland, R. Holzwarth, and F. Ö. Ilday, Nature (London) **537**, 84 (2016).
[22] L. V. Keldysh, Sov. Phys. JETP **20**, 1307 (1965) [Zh. Eksp. Teor. Fiz. **47**, 1945 (1964)].
[23] P. Liu, W. L. Smith, H. Lotem, J. H. Bechtel, N. Bloembergen, and R. S. Adhav, Phys. Rev. B **17**, 4620 (1978).
[24] V. Nathan, A. H. Guenther, and S. S. Mitra, JOSA B **2**, 294 (1985).
[25] R. DeSalvo, A. A. Said, D. J. Hagan, E. W. Van Stryland, and M. Sheik-Bahae, IEEE J. Quantum Electron. **32**, 1324 (1996).
[26] R. J. Elliott, Phys. Rev. **108**, 1384 (1957).
[27] R. Braunstein and N. Ockman, Phys. Rev. **134**, A499 (1964).
[28] A. Vaidyanathan, T. Walker, A. H. Guenther, S. S. Mitra, and L. M. Narducci, Phys. Rev. B **21**, 743 (1980).
[29] M. Kolesik and J. Moloney, Rep. Prog. Phys. **77**, 016401 (2014).
[30] W. V. Houston, Phys. Rev. **57**, 184 (1940).
[31] P. A. Zhokhov and A. M. Zheltikov, Phys. Rev. Lett. **113**, 133903 (2014).
[32] C. R. McDonald, G. Vampa, P. B. Corkum, and T. Brabec, Phys. Rev. Lett. **118**, 173601 (2017).
[33] E. O. Kane, J. Phys. Chem. Solids **1**, 249 (1957).
[34] V. N. Ostrovsky, T. K. Kjeldsen, and L. B. Madsen, Phys. Rev. A **75**, 027401 (2007).
[35] Y. V. Vanne and A. Saenz, Phys. Rev. A **75**, 033403 (2007).
[36] L. V. Keldysh, Sov. Phys. JETP **6**, 763 (1958) [Zh. Eksp. Teor. Fiz. **33**, 994 (1957)].
[37] J. B. Krieger, Phys. Rev. **156**, 776 (1967).
[38] A. M. Perelomov, V. S. Popov, and M. V. Terent'ev, Sov. Phys. JETP **23**, 924 (1966) [Zh. Eksp. Teor. Fiz. **50**, 1393 (1966)].
[39] S. V. Popruzhenko, P. A. Korneev, S. P. Goreslavski, and W. Becker, Phys. Rev. Lett. **89**, 023001 (2002).
[40] P. A. Korneev, S. V. Popruzhenko, S. P. Goreslavski, T.-M. Yan, D. Bauer, W. Becker, M. Kübel, M. F. Kling, C. Rödel, M. Wünsche, and G. G. Paulus, Phys. Rev. Lett. **108**, 223601 (2012).
[41] A. Dragonmir, J. G. McInerney, and D. N. Nikogosyan, Appl. Opt. **41**, 4365 (2002).
[42] S. A. Slattery and D. N. Nikogosyan, Opt. Commun. **228**, 127 (2003).
[43] K. J. Leedle, K. E. Urbanek, and R. L. Byer, Appl. Opt. **56**, 2226 (2017).
[44] The electron spin is taken into account.
[45] The 2PA coefficient of sapphire measured via the z-scan technique [25] at $\hbar\omega/\epsilon_g \approx 0.5$ (filled square) is roughly one order of magnitude above the values obtained via two-photon conductive sapphire sensor [43] (empty squares). This is explained by the "possible reduction in the measured current extraction due to carrier recombination."
[46] D. Waroquiers, A. Lherbier, A. Miglio, M. Stankovski, S. Poncé, M. J. T. Oliveira, M. Giantomassi, G.-M. Rignanese, and X. Gonze, Phys. Rev. B **87**, 075121 (2013).
[47] R. H. French, J. Am. Ceram. Soc. **73**, 477 (1990).
[48] G. G. Paulus, F. Grasbon, H. Walther, R. Kopold, and W. Becker, Phys. Rev. A **64**, 021401 (2001).
[49] H. Zimmermann, S. Patchkovskii, M. Ivanov, and U. Eichmann, Phys. Rev. Lett. **118**, 013003 (2017).
[50] I. H. Malitson, JOSA **55**, 1205 (1965).
[51] I. H. Malitson, JOSA **52**, 1377 (1962).